Available online at www.sciencedirect.com

ScienceDirect

journal homepage: www.elsevier.com/locate/watres

Phosphate and arsenate removal efficiency by thermostable ferritin enzyme from *Pyrococcus furiosus* using radioisotopes

Ana-Maria Sevcenco [a,b,c], *Monica Paravidino* [c], *Johannes S. Vrouwenvelder* [a,d], *Hubert Th. Wolterbeek* [b], *Mark C.M. van Loosdrecht* [a], *Wilfred R. Hagen* [a,*]

[a] *Department of Biotechnology, Delft University of Technology, Julianalaan 67, 2628 BC Delft, The Netherlands*
[b] *Department of Radiation, Radionuclides and Reactors, Delft University of Technology, Mekelweg 15, 2629 JB Delft, The Netherlands*
[c] *BiAqua B.V., Schipholweg 275, 1171 PK Badhoevedorp, The Netherlands*
[d] *King Abdullah University of Science and Technology, Water Desalination and Reuse Center, Thuwal, Saudi Arabia*

ARTICLE INFO

Article history:
Received 8 October 2014
Received in revised form
22 February 2015
Accepted 23 February 2015
Available online 13 March 2015

Keywords:
Ferritin
Arsenate
Phosphate
Biofouling control

ABSTRACT

Oxo-anion binding properties of the thermostable enzyme ferritin from *Pyrococcus furiosus* were characterized with radiography. Radioisotopes ^{32}P and ^{76}As present as oxoanions were used to measure the extent and the rate of their absorption by the ferritin. Thermostable ferritin proved to be an excellent system for rapid phosphate and arsenate removal from aqueous solutions down to residual concentrations at the picomolar level. These very low concentrations make thermostable ferritin a potential tool to considerably mitigate industrial biofouling by phosphate limitation or to remove arsenate from drinking water.

1. Introduction

In recent times interest in sustainable biotechnological techniques and their industrial application has increased, particularly in the water sector with a view to a predicted future crisis due to water shortage needed for agriculture, industry, human consumption and the environment. More than a billion people worldwide are in need of clean drinking water (Gleick, 1998). The problem is so vast that a single solution is not likely to work in every situation; therefore, there is room for various creative approaches. More than 2.2 million people die each year from preventable diseases caused by contaminated water (Gleick, 2002). The main pollutants are inorganic compounds (e.g. heavy metals), pathogens and organic compounds (Christensen et al., 1994). One important example is the arsenic contamination of groundwater, which has become a major problem for water supply in India and Bangladesh, causing serious arsenic poisoning to large numbers of people (Chowdhury et al., 2000). The World Health Organization

* *Corresponding author*. Tel.: +31 15 2785051; fax: +31 15 2782355.
E-mail address: w.r.hagen@tudelft.nl (W.R. Hagen).
http://dx.doi.org/10.1016/j.watres.2015.02.054

(WHO) recommends a maximum concentration of 10 μg/l as a health-based provisional guideline value for arsenic in drinking water (World Health Organization, 2011). There are techniques available to deal with this problem, but none of them prove to be sustainable. In this work we present a potentially sustainable bio-based adsorption method to clean arsenic contaminated water using the thermostable enzyme ferritin from *Pyrococcus furiosus*.

Microorganisms exist naturally in aquifer and surface water systems. Any aquifer with a low organic content, even when considered pristine, will have some degree of bacteriological activity, and some of these organisms are opportunistic pathogens. In surface water pathogens are a major pollutant causing diseases. To protect drinking water from disease–causing microorganisms, water suppliers often add a disinfectant to drinking water like chlorine (Richardson et al., 1998). The presence of microorganisms in the water is normal but can have an important impact on industry. Most of these microorganisms are able to adhere to surfaces and to produce an exopolymeric substance matrix to form a microbial biofilm that can act as a barrier protecting the bacteria incorporated in the films from harmful substances such as disinfectants (Winter et al., 1998). Biofilms can cause important damage in water supply, food and pharmaceutical industries and in healthcare. There are multiple strategies aiming to prevent or remove biofouling, e.g., chemical, mechanical, ultrasonic cleaning. However, in most of these cases the industrial process needs to be shut down, and the down time is expensive, or decreases the life span of the system. Therefore, we present a milder and sustainable way of preventing biofouling with potential for industrial application. Thermostable ferritin from *P. furiosus* has been shown to remove orthophosphate PO_4^{3-} from water (Jacobs et al., 2010) and therefore to limit available nutrients that could help the biofilm to develop. Orthophosphate limitation has been shown to be a method to control biofouling: low phosphate concentrations (~0.3 μg P/L) in the feed water restrict biomass accumulation in industrial membranes even at high biodegradable substrate (organic carbon) concentrations (Miettinen et al., 1997; Vrouwenvelder et al., 2010).

Ferritin is an iron storage protein that is universally found in prokaryotes and eukaryotes. Prokaryotic ferritin consists of 24 identical subunits that are assembled in a roughly spherical protein with an outer diameter of approximately 12 nm and inner cavity diameter of 8 nm. In its nanocage the ferritin from the hyperthermophilic archaeon *P. furiosus* can form a hydrated iron oxide mineral core of up to circa 2700 ferric ions, whereas higher loading results in destabilization and precipitation of the protein (Matias et al., 2005). The *P. furiosus* ferritin structural gene can be expressed to high levels in *Escherichia coli* and the recombinant protein can be very easily purified (Tatur et al., 2006), making it suitable for large–scale production. The ferritin is stable and active at 100 °C for 10 h and it resists sterilization at 121 °C for 30 min without loss of enzymatic activity (Matias et al., 2005). Ferric iron nanoparticles encapsulated in a ferritin nanocage act as a sorbent for orthophosphate, forming an iron–oxyhydroxide–phosphate nanoparticle. The mineral core can be regenerated by release of phosphate after iron reduction (Harrison and Arosio, 1996). In addition to PO_4^{3-} this protein has a high capacity for removal of other oxoanions such as arsenate AsO_4^{3-} or vanadate VO_4^{3-} (Honarmand Ebrahimi et al., 2010).

In initial sorption experiments of PO_4^{3-} Jacobson et al. (2009) had no analytical tool available to directly measure how efficiently ferritin removes oxoanions from water. In the present study we have addressed this problem by characterizing the capacity removal of ferritin using radioisotope labeled phosphate and arsenate solutions, $^{32}PO_4^{3-}$ and $^{76}AsO_4^{3-}$. This proved to be an extremely sensitive analytical approach that can trace ppt (ng/L) level concentrations. Results of this study indicate that ferritin can attain an effective phosphate removal capacity of approximately 11 mg PO_4^{3-}/g ferritin and 7 mg AsO_4^{3-}/g ferritin.

2. Materials and methods

2.1. Ferritin solution

The recombinant ferritin from *P. furiosus* has been expressed in a proprietary *E. coli* strain, produced in batch fermentation, and purified by heat treatment in a pilot (1000 g ferritin) for scale-up to future production for industrial applications, by DSM, Delft, The Netherlands. The protein sample purity (>70%) was verified by SDS gel electrophoresis.

2.2. Regeneration

Purified ferritin was buffer–exchanged into a working buffer of 100 mM 3–(N–morpholino) propanesulfonic acid (MOPS) at pH 7.0. Regeneration of the ferritin was done according to Jacobs et al. (2010) using sodium dithionite as reductant. The iron ions released from the core were chelated with sodium ethylenediaminetetraacetic acid (EDTA). The molar ratio to obtain apo-ferritin (i.e. free of iron) was 1 μmol ferritin: 3.33 mmol Na–dithionite: 1.65 mmol EDTA. Na–dithionite and EDTA were removed from the solution by washing with buffer. Protein concentration was measured using the bicinchoninic acid method.

2.3. Iron incorporation

Freshly prepared anaerobic ferrous sulfate solutions were used for loading the apo-ferritin, according to Jacobs et al. (2010). The mineralized ferritin core was formed by stepwise addition of appropriate amounts of Fe^{2+} while stirring at room temperature. After each addition the sample was left for 5 min to allow for the Fe^{2+} incorporation and enzymatic oxidation to Fe^{3+} with air. 2500 iron molecules were maximally incorporated in one ferritin molecule.

2.4. ^{32}P and ^{76}As production

^{32}P–labeled diammonium phosphate $(NH_4)_2HPO_4$ and ^{76}As–labeled As_2O_5 were prepared at the Reactor Institute Delft (Delft University of Technology, The Netherlands). A short description of each radioisotope production and stock solution preparation is presented below.

Preparation of ^{32}P solution – Radioisotope ^{32}P ($t_{1/2}$ = 14.28 d) was obtained by irradiation for 100 h of a sealed quartz tube

containing 2 mg highly pure $(NH_4)_2HPO_4$ using fast neutrons (3.7×10^{17} m^{-2} s^{-1}). After a 60 h cooling time a specific activity of 20.60×10^9 Bq/g was obtained. The irradiated material was dissolved in 10 ml Milli–Q water to a stock solution of 1.4 mM ^{32}P–spiked PO_4^{3-} from now on referred to as $^{32}PO_4^{3-}$.

Preparation of ^{76}As solution – Pentavalent radioisotope ^{76}As ($t_{1/2}$ = 1.10 d) was obtained by 1 h irradiation of a sealed quartz tube containing 2 mg As_2O_5 using fast neutrons (3.7×10^{17} $m^{-2}s^{-1}$). After a 30 h cooling time a specific activity of 2.15×10^{10} Bq/g was obtained. The irradiated material was dissolved in 10 ml Milli–Q water to a stock solution of 1.7 mM ^{76}As–spiked AsO_4^{3-} from now on referred to as $^{76}AsO_4^{3-}$.

2.5. *Adsorption experiments*

Adsorption experiments were carried out as batch liquid–liquid phase equilibrations. Volumes of 10 ml solution of radioactively labeled solute $^{32}PO_4^{3-}$ or $^{76}AsO_4^{3-}$ were equilibrated with ferric iron loaded ferritin solution. The system was left to reach equilibration overnight. Aqueous oxoanion solution and ferritin were separated using a Millipore filter with 3 kDa cut off. The $^{32}PO_4^{3-}$ or $^{76}AsO_4^{3-}$ concentration that remained in the permeate after reaching equilibrium was quantified by measuring the β^- radiation emission using a liquid scintillation counter (LSC) Tri–Carb 2750TR/LL (Packard, Meriden, USA). The reaction with apo-ferritin in the absence of iron was taken as the blank measurement. Before counting, each aqueous sample was mixed in a 1:1 ratio with Ultra Gold XR™ LSC cocktail (PerkinElmer, Boston, USA) giving a final volume of 20 ml.

3. Results

3.1. *Adsorption isotherm of $^{32}PO_4^{3-}$ by ferritin solution*

There are basically two ways of phosphate incorporation into ferritin: simultaneously (i.e. Fe(II) and phosphate at once) or sequentially (i.e. first Fe(II) and then phosphate). Previous work has shown that there is a circa six–fold difference between the phosphate removal capacities under the two conditions, sequential loading has a sorption of 0.1 mol PO_4^{3-}/mol Fe and simultaneous loading has a phosphate binding capacity of 0.6 mol PO_4^{3-}/mol Fe (Jacobs et al., 2010). A schematic outline of these two modes is re-drawn in Fig. 1 A and B, and is here extended with a refinement (Fig. 1C) in which the hydrated iron oxide core grows from more than one nucleation site.

Fig. 2A presents the phosphate removal capacity when the ferritin is sequentially loaded with iron and phosphate using variable amounts of iron. The data are fitted to a shifted Langmuir isotherm

$$y = \frac{c_1 \cdot (x - 48)}{c_2 + x - 48} \quad (1)$$

in which y is the phosphate bound per ferritin (mg/g), x is the iron loaded per ferritin in mol/mol, c_1 is the saturation value of bound phosphate per ferritin in mg/g (multiply by 5.0 to convert to mol/mol)), c_2 is an effective dissociation constant (mol/mol iron per ferritin for half-saturated phosphate binding), and the 48 Fe per ferritin shift is to account for the fact that the first 48 Fe added to apo-ferritin occupy the 24 dinuclear ferroxidase catalytic centers in the 24 subunits, and do not contribute to phosphate-binding capacity (Honarmand Ebrahimi et al., 2010). The total added phosphate concentration in this experiment is constant, while the iron concentration in ferritin is varied. The fact that the data can be fitted to equation (1) suggests that the amount of phosphate bound is proportional to the amount of iron, which would imply that the coordination chemistry of the iron–phosphate complex does not drastically vary with increasing occupancy of the core surface by phosphate.

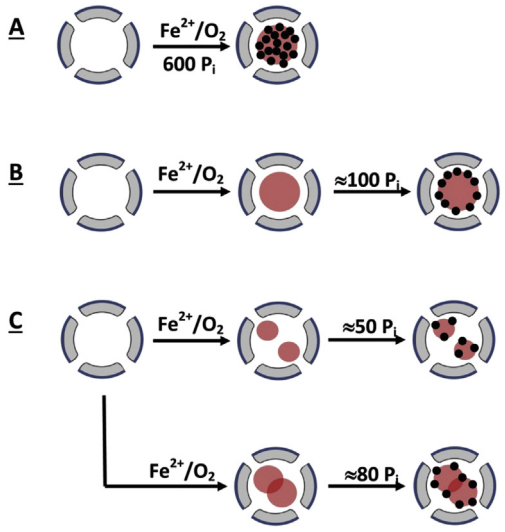

Fig. 1 – Phosphate binding to ferritin. Schematic representation of binding patterns of phosphate to ferritin containing circa 1000 Fe per enzyme molecule: (A) simultaneous loading leading to homogeneous incorporation of phosphate into the core; (B) sequential loading leading to surface adsorption of phosphate onto the core; (C) sequential loading with core formation from more than one nucleation site. Given phosphate/ferritin stoichiometries are indicative values.

In Fig. 2B the data are replotted as binding-efficiency numbers, i.e. ratios of phosphate-bound per iron. The solid traces are power-law fits to the data according to

$$y = c_S \cdot (x - 48)^{c_E} \quad (2)$$

in which c_S is a scaling factor. The blue line is a fit with the exponential fixed at $c_E = -1/3$; the green line is a fit with the exponential as a free fitting parameter affording $c_E = -0.43 \pm 0.03$. An exponential of $-1/3$ would be predicted by the simple sequential-loading model of Fig. 1B, in which the stored iron forms a single ideal sphere whose surface is exclusively available for the binding of phosphate. The power of $-1/3$ reflects the slower increase in surface versus increase in volume of a growing sphere. The observation that the efficiency decays even more rapidly indicates that the model of a single, homogeneously growing core (cf Fig. 1B) is perhaps too simple and should be adjusted to include the possibility of several nucleation sites for core formation as schematically depicted in Fig. 1C.

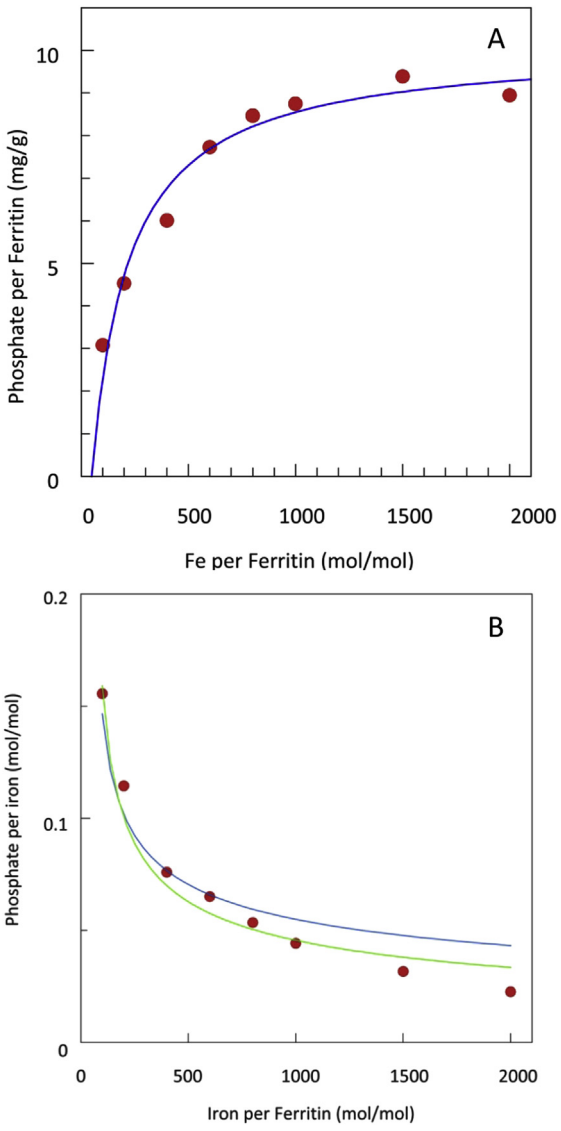

Fig. 2 – Phosphate removal capacity of ferritin. A: Phosphate removal capacity after different iron loading steps for sequential loading. The data has been fitted to equation (1) with saturation value $c_1 = 10.11 \pm 0.44$ mg/ml and dissociation constant $c_2 = 174 \pm 33$ Fe/ferritin. B: Dependence of the core size on the PO_4^{3-}/Fe ratio in sequential loading. The fits to the data are according to equation (2) with $c_S = 0.54 \pm 0.03$ and $c_E \equiv -1/3$ (upper trace) or $c_S = 0.87 \pm 0.15$ and $c_E = -0.43 \pm 0.03$.

A simple adsorption isotherm

$$y = \frac{c_1 \cdot x}{c_2 + x} \tag{3}$$

for sequential loading of PO_4^{3-} was determined on ferritin loaded with 1500 Fe ions. The result in Fig. 3 is presented as a dose–response curve, i.e. with the added ligand concentration on a log scale. The maximum removal capacity achieved is 12.3 ± 0.3 mg PO_4^{3-}/g ferritin, and the apparent dissociation constant is 1.14 ± 0.12 μM phosphate.

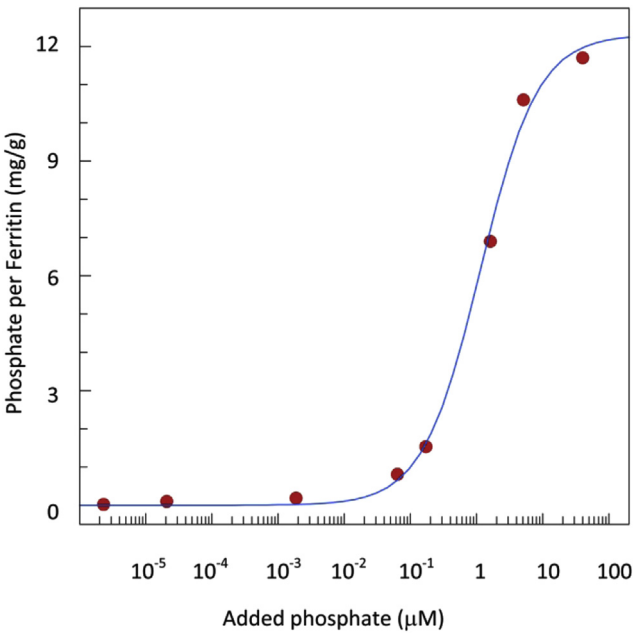

Fig. 3 – Phosphate sorption on ferritin. 70 nM ferritin loaded with 1500 Fe molecules per ferritin core has been exposed to various phosphate concentrations and left for 24 h to reach equilibrium. The solid line is a fit to equation (3) with saturation value $c_1 = 12.31 \pm 0.30$ mg/g phosphate/ferritin and dissociation constant $c_2 = 1.14 \pm 0.12$ μM phosphate.

Fig. 4A shows that for a fixed iron loading of 1500 Fe per ferritin the phosphate removal capacity is decreasing when the PO_4^{3-} concentration is increasing. To make sure equilibrium was reached, the reaction was monitored for 24 h. In Fig. 4B the time dependency to reach equilibrium is shown. It is seen that within 10 min more than 97% of the phosphate is incorporated in the ferritin, while the remaining 3% is slowly binding to the ferritin core in time. The solid trace in Fig. 4B is a two-exponential fit to the data according to equation (4)

$$y = A_1 \cdot \left(1 - e^{-r_1 x}\right) + A_2 \cdot \left(1 - e^{-r_2 x}\right) \tag{4}$$

with amplitudes $A_1 = 96.3 \pm 0.4\%$ and $A_2 = 3.2 \pm 0.4\%$. For the fast and the slow phase, respectively, the rate constants are $r_1 = 78 \pm 35\ h^{-1}$ and $r_2 = 1.4 \pm 0.4\ h^{-1}$. A molecular basis for this two-phase behavior is yet to be determined, but the practical bottom line is that adsorption of phosphate by ferritin occurs on a minutes time scale when the system is run at or below circa 97% of its maximal capacity.

3.2. *Adsorption isotherm of $^{76}AsO_4^{3-}$ by ferritin solution*

Fig. 5 shows the isotherm of $^{76}AsO_4^{3-}$ adsorption to the ferritin. Different concentrations of radiolabeled oxoanion $^{76}AsO_4^{3-}$ have been equilibrated with ferritin containing 1500 iron molecules in the mineral core. 7 mg AsO_4^{3-}/g ferritin was the maximum arsenic removal capacity that was achieved when the core was formed out of 1500 Fe ions per ferritin.

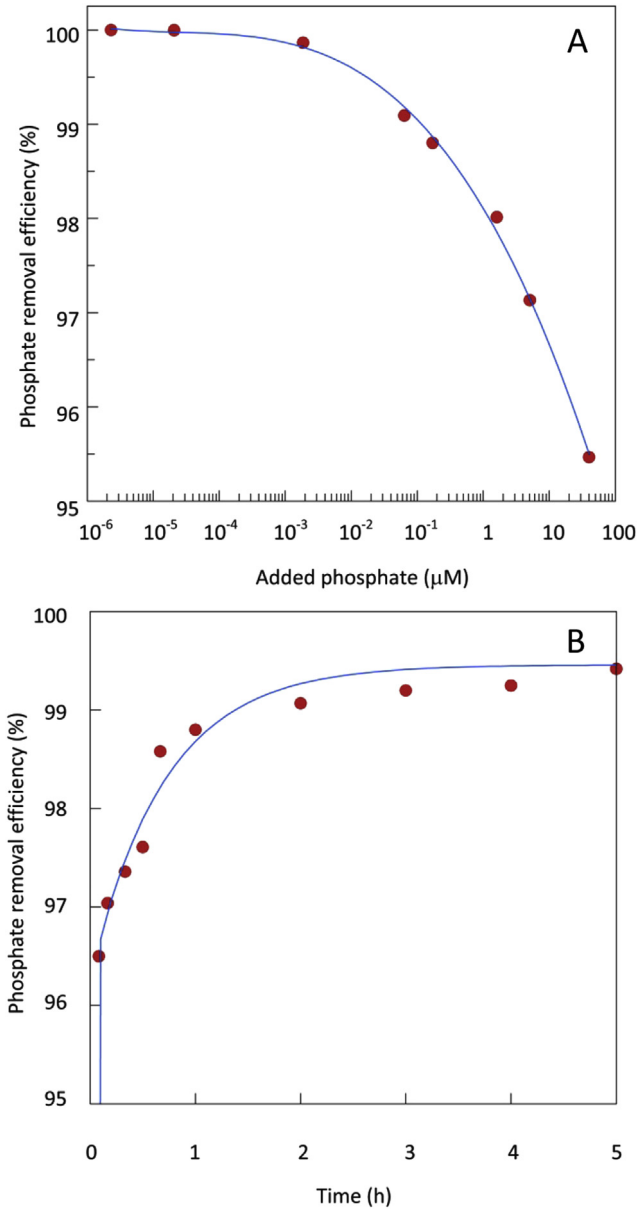

Fig. 4 – Phosphate removal efficiency of ferritin. A: Phosphate removal efficiency of 70 nM ferritin loaded with 1500 Fe molecules per ferritin core at various phosphate concentrations. The reaction was done at room temperature for 24 h. The data has been fit to a third-order polynomial. B: Phosphate removal efficiency in time: 70 nM ferritin loaded with 1500 Fe molecules was treated with 50 nM $^{32}PO_4^{3-}$ giving rise to a dominant fast phase and a minor slow phase.

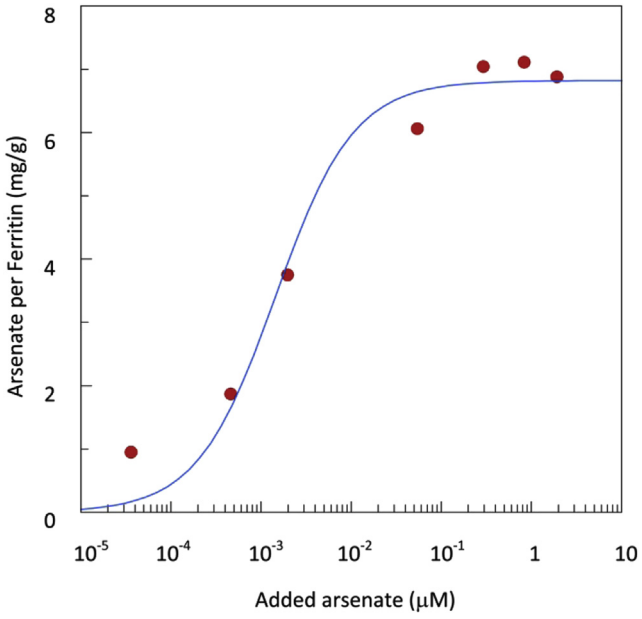

Fig. 5 – Arsenate sorption on ferritin. 1 μM ferritin loaded with 1500 Fe molecules per ferritin core has been exposed to various $^{76}AsO_4^{3-}$ concentrations and left for 24 h to reach equilibrium. The data has been fit to a Langmuir isotherm in equation (3) with saturation value $c_1 = 6.82 \pm 0.25$ mg/g arsenate/ferritin and dissociation constant $c_2 = 1.45 \pm 0.36$ nM arsenate.

4. Discussion

Iron oxides and hydroxides in aerobic environments have strong adsorption capacity for orthophosphate and arsenate. The ferritin mineral iron core is associated with phosphate sorption, forming an iron–oxyhydroxide–phosphate nanoparticle core. To measure the exact adsorption capacity of ferritin, radiolabeled $^{32}PO_4^{3-}$ and $^{76}AsO_4^{3-}$ solutions have been used. Based on the results presented above, ferritin proved to have an excellent phosphate and arsenic adsorption capacity. Its capability of removing these oxoanions from the water to residual pM levels underlines the potential of ferritin as a material for use in production of clean drinking water or process water. In case of phosphate removal it has been shown that orthophosphate limitation is a method to control biofouling (Vrouwenvelder et al., 2010). Low phosphate concentrations (~0.3 μg P/L) in the feed water restrict biomass accumulation in industrial membranes even at high substrate (organic carbon) concentrations. Our results show that ferritin was able to remove phosphate from the water well below this value. Using membrane fouling simulators (MFS) systems (Miettinen et al., 1997; Jacobson et al., 2009; Vrouwenvelder et al., 2006) we found that sequentially loaded ferritin afforded a time delay in the biofouling build up by a factor three (our unpublished observations).

The World Health Organization has recommended 5–10 μg/l as a health-based guideline value for arsenic in drinking water (WHO, 2011). With ferritin we have measured reduction to pM levels, which is a thousand fold below the guideline. When 10 μg/l arsenic level is allowed in tap water the approximate total risk of cancer to occur is estimated to be 1 in 500 people, with the assumption that an individual drinks 2 L of tap water per day (Khedr, 2000). Our data indicate that one could limit the arsenic concentration to values where the risk of cancer occurrence would decrease to 1 in 100 000 individuals. Arsenic removal technologies are in general complex, not sustainable, costly, and in many cases not capable of consistently removing all forms of arsenic down to the desired

level of 10 μg/L. Such technologies include enhanced coagulation followed by flock separation either through sedimentation or membrane filtration, lime softening, reverse osmosis and nano-filtration, filtration through manganese-green sand filter, and in-situ subsurface removal (Ali et al., 2011). Adsorption is recognized as an efficient and economical method of water treatment (Mohan and Pittman, 2007). Our ferritin-based adsorption technique could be envisioned to be implemented as a downstream polishing step for traditional arsenic removal technologies.

5. Conclusions

We have determined the characteristics for phosphate and arsenate uptake by thermostable ferritin. The use of radioisotope labelled phosphate and arsenate solutions, $^{32}PO_4^{3-}$ and $^{76}AsO_4^{3-}$, proved to be a very sensitive analytical approach that afforded trace ppt (ng/L) level concentration determinations, giving us an accurate picture on the phosphate and arsenate absorption capacity of ferritin. A high affinity for both oxyanions has been established underlining the potential of thermostable ferritin as a material for use in production of clean drinking water and process water.

REFERENCES

Ali, I., Khan, T.A., Hussain, I., 2011. Treatment and remediation methods for arsenic removal from the ground water. Int. J. Environ. Eng. 3 (1), 48–71.

Chowdhury, U.K., Biswas, B.K., Chowdhury, T.R., Samanta, G., Mandal, B.K., Basu, G.C., Chanda, C.R., Lodh, D., Saha, K.C., Mukherjee, S.K., Roy, S., Kabir, S., Quamruzzaman, Q., Chakraborti, D., 2000. Groundwater arsenic contamination in Bangladesh and West Bengal, India. Environ. Health Perspect. 108 (5), 393–397.

Christensen, T.H., Kjeldsen, P., Albrechtsen, H.–J., Heron, G., Nielsen, P.H., Bjerg, P.L., Holm, P.E., 1994. Attenuation of landfill leachate pollutants in aquifers. Crit. Rev. Environ. Sci. Technol. 24 (2), 119–202.

Gleick, P.H., 1998. The human right to water. Water Policy 1, 487–503.

Gleick, P.H., 2002. Dirty Water: Estimated Deaths from Water-related Disease 2000–2020. Pacific Institute Research Report. http://www.pacinst.org/reports/water_related_deaths/water_related_deaths_report.pdf.

Harrison, P.M., Arosio, P., 1996. Ferritins: molecular properties, iron storage function and cellular regulation. Biochim. Biophys. Acta 1275 (3), 161–203.

Honarmand Ebrahimi, K., Hagedoorn, P.-L., Hagen, W.R., 2010. Inhibition and stimulation of formation of the ferroxidase center and the iron core in *Pyrococcus furiosus* ferritin. J. Biol. Inorg. Chem. 15 (8), 1243–1253.

Jacobs, J.F., Hasan, M.N., Paik, K.H., Hagen, W.R., van Loosdrecht, M.C.M., 2010. Development of a bionanotechnological phosphate removal system with thermostable ferritin. Biotechnol. Bioeng. 105 (5), 918–923.

Jacobson, J.D., Kennedy, M.D., Amy, G., Schippers, J.C., 2009. Phosphate limitation in reverse osmosis: an option to control biofouling? Desalin. Water Treat. 5 (1–3), 198–206.

Khedr, G., 2000. Membrane fouling problems in reverse osmosis desalination applications. Desalin. Water Reuse 10, 3–10.

Matias, P.M., Tatur, J., Carrondo, M.A., Hagen, W.R., 2005. Crystallization and preliminary X-ray characterization of a ferritin from the hyperthermophilic archaeon and anaerobe *Pyrococcus furiosus*. Acta Crystallogr. Sect. F. 61 (5), 503–506.

Miettinen, I.T., Vartiainen, T., Martikainen, P.J., 1997. Phosphorus and bacterial growth in drinking water. Appl. Environ. Microbiol. 63 (8), 3242–3245.

Mohan, D., Pittman Jr., C.U., 2007. Arsenic removal from water/wastewater using adsorbents – a critical review. J. Hazard. Mater. 142 (1–2), 1–53.

Richardson, S.D., Thruston Jr., A.D., Caughran, T.V., Collette, T.W., Patterson, K.S., Lykins Jr., B.W., 1998. Chemical by-products of chlorine and alternative disinfectants. Food Technol. 52 (4), 58–61.

Tatur, J., Hagedoorn, P.-L., Overeijnder, M.L., Hagen, W.R., 2006. A highly thermostable 1 ferritin from the hyperthermophilic archaeal anaerobe *Pyrococcus furiosus*. Extremophiles 10 (2), 139–148.

Vrouwenvelder, J.S., van Paassen, J.A.M., Wessels, L.P., van Dam, A.F., Bakker, S.M., 2006. The membrane fouling simulator: a practical tool for fouling prediction and control. J. Membr. Sci. 281 (1–2), 316–324.

Vrouwenvelder, J.S., Beyer, F., Dahmani, K., Hasan, N., Galjaard, G., Kruithof, J.C., van Loosdrecht, M.C.M., 2010. Phosphate limitation to control biofouling. Water Res. 44 (11), 3454–3466.

Winter, T.C., Harvey, J.W., Franke, O.L., Alley, W.M., 1998. Ground Water and Surface Water – a Single Resource. U.S. Geological Survey Circular, p. 1139. http://pubs.usgs.gov/circ/circ1139/pdf/circ1139.pdf.

World Health Organization, 2011. Arsenic in Drinking Water: Fact Sheet 210 (Revised) May 2011. http://apps.who.int/inf-fs/en/fact201.html.